Integrated Nano, 2024, Vol. X, Iss. X, 27-40

DOI: 10.62184/in.jin0101202422

Research Article

SCIENCE PARK PUBLISHER

Integrated Nano

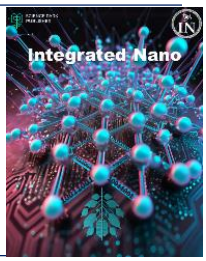


# Airflow sensing and energy harvesting applications of PVDF-TPU piezoelectric nanofibers

**Remya Nair[1,2*], Omar Amjad[2], Ankur Jain[3]**

[1] School of Applied Sciences, Suresh Gyan Vihar University Jaipur

[2] Kuwait College of Science and Technology, Doha Area, 7th Ring Road, Safat 13133, Kuwait

[3] Centre for Renewable Energy & Storage, Suresh Gyan Vihar University, Jaipur

**Received: 24, 12, 2023; Accepted: 21, 04, 2024; Published: 10, 07, 2024**



## Abstract

Wind energy is one of the abundant potential power sources that can be found both indoors and outdoors. Recently, the focus has been placed on the potential of ambient energy gathering using natural airflow as a small-scale wind energy source. Here, highly piezoelastic nanofiber mats were fabricated from a pure polyvinylidene fluoride (PVDF) and PVDF-TPU (thermoplastic polyurethane) composites via the electrospinning approach. They have exceptional electrical energy harvesting and airflow sensing capabilities. The potential of these composite nanomats for piezoelectric energy harvesting was studied, depending on airflow perturbations in the surrounding environment. PVDF blended with 15 weight percent (wt.%) TPU exhibited the optimum sensitivity, clearly demonstrating the scope of these developed prototypes in the field of airflow sensing and energy harvesting technology.

**Keywords:** Electrospinning; Ambient Energy; Wind Energy Harvesting; Piezoelastic; Airflow Sensor; PVDF-TPU Piezoelectric Nanofiber Prototype

## 1. Introduction

Global population growth and urbanization have increased electricity demand, necessitating a shift towards renewable energy sources like solar, wind, and sound energy. This not only meets energy requirements but also reduces greenhouse gas emissions, impacting climate and weather conditions [1–3]. When it comes to nonconventional energy resources, ambient energy harvesting is a significant field that has lately evolved to make use of the unused energy present in the environment. Ambient energy refers to any form of energy available in the environment for electrical energy generation. It can be natural, such as heat and wind energy, or artificial, such as human activities or devices [4]. The creation of specific novel prototypes can lead to the use of this ambient energy that is now underutilized. These widely available power sources have the potential to enable real-time energy harvesting and storage for later use, making them an alternative to conventional batteries. We mostly rely on locally accessible energy sources for energy collection, and the energy produced is used for local applications where a small amount of energy is sufficient to meet the need. To activate wireless sensors, for instance, we may use this energy [5]. Environmental energy harvesting converts ambient energy into electricity due to its small volume, extended lifespan,

Integrated Nano, 2024, Vol. X, Iss. X, 27-40
DOI: 10.62184/in.jin0101202422

Research Article

and high energy density. This requires sophisticated technology and procedures. Common transduction mechanisms include photoelectric, thermoelectric, induction, piezoelectric, and electromagnetic effects. Our study focuses on converting environmental airflow or motion-based energy sources into electrical energy, including wind and airflow in everyday life [6]. Through the vibrational energy harvesting technique of airflow excited piezoelectric energy harvesting, structural vibrations are converted into electrical energy [7]. The three primary energy transduction mechanisms for motion-based or vibrational movements are piezoelectric, electrostatic, and electromagnetic effects. Our area of interest and concern among these effects is the transmission mechanism based on piezoelectricity. Piezoelectric technology is making its way into the field of sensing systems and energy harvesting [8].

Piezoelectric energy harvesting is a sophisticated technology using smart materials like piezoelectric materials for mechanical energy-based ambient energy collection. Mechanical stress produces electrical energy, while electrical disturbances cause mechanical deformation, resulting in charge separation and voltage production [9]. The direct piezoelectric effect formula can be used to represent a material's piezoelectric activity and is given by:

$$\mathbf{D = d\,T + \varepsilon\,E} \qquad (\mathbf{1})$$

The displacement is represented by "D", the applied mechanical stress is denoted by "T", the material permittivity is indicated by "ε", the piezoelectric coefficient is shown by "d", and the electric field is indicated by "E". The material with a higher piezoelectric coefficient value "d" produces a greater piezoelectric voltage for a given amount of applied mechanical stress [10].

Piezoelectric materials fall into three primary categories, such as polymers, ceramics, and crystals. Comparing polymeric piezoelectric materials to other piezoelectric materials, they are less brittle, less poisonous, and more mechanically stable with flexibility, which makes them perfect for ambient energy collection [11]. The remarkable mechanical stability and customizable electrical properties of nanoscale-based piezoelectric polymer materials, along with their high porosity and surface-to-volume ratio, make them highly effective in producing electrical signals even from minute physical changes [12]. Any nanostructured material that may use the piezoelectricity principle to convert external kinetic energy into an electrical potential or electrical energy is defined as a piezoelectric nanogenerator [13]. To capture underutilized mechanical energy present in the environment, piezo-active nanofiber mats fabricated via the electrospinning technique are utilized as the primary medium in the current study. Excellent piezo-stability in polymer-based nanofiber membranes is primarily attained through the electrospinning method. Here, a stronger electric field is used to create nanofibers by utilizing electrostatic repulsion forces [14]. Electrospinning involves electrifying a liquid droplet to create a jet, which is stretched and extended to create fibers. The polymer solution is loaded onto a syringe, controlled by an injection pump, and kept at a specific distance from a rotating drum collector. The main source for electrification is a high-voltage power supply. The liquid droplet undergoes electrification when a high-voltage power supply is turned on, forming a Taylor cone with small jets due to its high charge density. These jets stretch and extend, forming elongated ultrafine filaments [15].

Our primary choice of polymer associated with environmental airflow energy harvesting in the current study is PVDF, which is one of the best piezoelectric polymers with a piezoelectric coefficient value in the range of 20–40 pC/N. The advantages of PVDF and its copolymers are numerous and include excellent halogen and acid resistance, good biocompatibility, good flexibility, and environmental friendliness. PVDF is an excellent option for piezoelectric applications due to its polar crystalline structure, which produces high voltages at low strains [16]. Long chain molecules of the semicrystalline thermoplastic fluoropolymer PVDF $[C_2H_2F_2)_n]$ are created when vinylidene difluoride ($CH_2 = CF_2$) monomer units are polymerized. It is a 50–60 % crystallinity non-reactive polymer that is extremely stable. Because PVDF is polymorphic, it typically appears in five crystalline phases: α, β, γ, δ, and ε. The most common polymorphic phases in this case are α, β, and γ, with β-phases,

which draws the attention due to its piezoelectric properties [17]. The piezoelectric response of the polymeric PVDF is solely attributed to the β-phase. Several intriguing features of PVDF are produced by the distinct spatial configurations of the $CH_2$ and $CF_2$ groups along the polymer chain. About 3 wt.% of PVDF is hydrogen, and 59.4 wt.% is fluorine. The fluorine level of PVDF has a significant impact on the chemical and electrical characteristics of materials. PVDF molecules contain an internal dipole moment due to the presence of electronegative fluorine and electropositive hydrogen [18]. The β polymorph has an orthorhombic crystallographic system with all trans-trans (TTTT) molecular conformations [19]. The β-phase's all TTTT planar zigzag molecule shape produced a non-zero net dipole moment, and the C-F dipoles and C-C chain backbone are arranged in such a way that they cancel out each other [20].

PVDF nanofibers are used in sensor technologies and energy harvesting, among other smart system applications. [21]. Systems that need the measurement or detection of contact use a primary type of PVDF sensor known as a tactile sensor. For sensing pulses and physiological signals in medical applications (e.g., heart rate and respiratory cycle monitoring), PVDF tactile sensors are perfect choice [22]. Due to their fast reaction times and high sensitivity to physical strain, they are perfect for teleoperations and the prevention of diseases that require constant body monitoring [23]. Also, they are used to detect damage to structurally significant components in complicated systems. After being appropriately built and equipped to fit the curvature and shape of each component, the PVDF can be applied to the surfaces of the pipes, ducts, beams, and other components [24]. The sensor can then measure the change in strain to identify any damage, such as a crack [25]. PVDF and piezoelectric sensors have the advantage of being self-excited, which lowers their costs as they don't need an external power source to function. Owing to its great sensitivity, the sensor has been demonstrated in experiments to accurately detect not just contact force but also the tactile "smoothness" of various materials, which is similar to our fingers' tactile sense [26]. Flow velocity measurements are a significant additional application for PVDF sensors since the voltage they produce is directly proportional to the airflow velocity [27]. It has been demonstrated that the force exerted by the gas on the nanofiber is dependent on the airflow velocity's second power [28, 29]. The breath airflow of patients with sleep apnea can be measured with this kind of sensor, which is similar to high-end pneumotachographs [30].

The abovementioned applications of PVDF clearly prove the scope of these polymer and polymer-based composites in the field of small-scale wind energy harvesting and airflow sensing applications [28-35]. Some studies have proven the scope of lead zirconate titanate (PZT) in the field of airflow sensing based on piezoelectricity [36]. The sensing and energy generation capabilities of the PVDF nanostructures can be enhanced by the addition of certain dopants or nanofillers along with the PVDF solution during the electrospinning process [37]. Some of the most common additives used with PVDF to enhance the piezoelectric response include zinc oxide (ZnO), graphene nanosheets, carbon nanotubes (CNTs), copper nanoparticles, PZT, etc. [38–42]. In addition, the β-phase content of the PVDF-based nanofibers was increased by certain compositions based on polymers. Thus, combining TPU with PVDF for electrospinning is an efficient way to develop electrospun nanomembranes with excellent piezoelectric and pyroelectric properties with the advantage of the elastomeric properties of TPU [43]. TPU is a very adaptable elastomer with special qualities that provide excellent processing flexibility and stretchability in addition to excellent performance. TPU is a special kind of plastic that bridges the gap between plastic and rubber. A TPU is a block copolymer made up of hard and soft segments arranged in alternating order [44]. The hard parts are isocyanates; depending on the kind, they might be categorized as aromatic or aliphatic. The reacted polyol is what makes up the soft segments. The qualities of the resulting TPU are determined by the type of isocyanate and polyol, in addition to the ratio of hard to soft segments in a certain grade of TPU [45]. A different study evaluated the impact of incorporating TPU with PVDF nanofibers on mechanical and piezoelectric capabilities [46].

Integrated Nano, 2024, Vol. X, Iss. X, 27-40

DOI: 10.62184/in.jin0101202422

Research Article

Most of the studies lacks the utilization of PVDF and PVDF composite-based nanofibers utilization in the field of airflow sensing and wind energy harnessing. The present study deals with the behavior of electrospun PVDF and PVDF-TPU-based nanomats on the uniform airflow as a part of their scope in small-scale wind energy harvesting technology.

## 2. Experimental Methodology

### 2.1. Materials

Polyvinylidene (PVDF, Kynar®, King of Prussia, PA, USA) with molecular weight (Mwt) = 444, 000 g/mol was supplied by Arkema. Thermoplastic polyurethane (TPU, BASF Co., Ltd., Berlin, Germany) was purchased with a Mwt= 107, 020 g/mol and a polydispersity index (PDI) of 1.83. Dimethylformamide (DMF, 98%, Sigma Aldrich, Taufkirchen, Germany) was used as a solvent for the preparation of the polymer solution. A 10 wt.% PVDF solution was prepared by dissolving 1 gram (g) of PVDF powder in ten milliliters (ml) of DMF. Also, a 10 wt.% TPU polymer solution was made by mixing 1 g of TPU pellets in 10 ml of DMF. Three different compositions of PVDF-TPU were prepared by adding 5, 10, and 15 wt.% of TPU to a pure PVDF solution. The preparation methods associated with the polymer compositions were identical to the ones that we used in our previous work on stretchable electrospun PVDF-TPU-based nanofiber [46, 49]. All four compositions (i.e., pure PVDF, PVDF-TPU 5 wt.%, PVDF-TPU 10 wt.%, and PVDF-TPU 15 wt.%) were fabricated, and their solutions were electrospun for the fabrication of nanofibers [46].

### 2.2. Methods

The PVDF-TPU nanofibers in our study are fabricated using the traditional electrospinning process setup, as shown in Figure 1. It is composed of an injection pump (NE1000-Single Syringe Pump, New Era, Farmingdale, New York, NY, USA) that controls the flow rate of the sample solution at 1.5 ml/hr. Also, it contains an 18-gauge metallic needle with a purely circular opening at the tip; a plastic syringe with a capacity of 10 ml; and a revolving collector coated in aluminium foil fixed 15 cm away from the needle tip. A positive high-voltage in the order of 25 kV is applied to the metallic needle using a high-voltage power supply from Divotech (30 kV/1.65 mA).

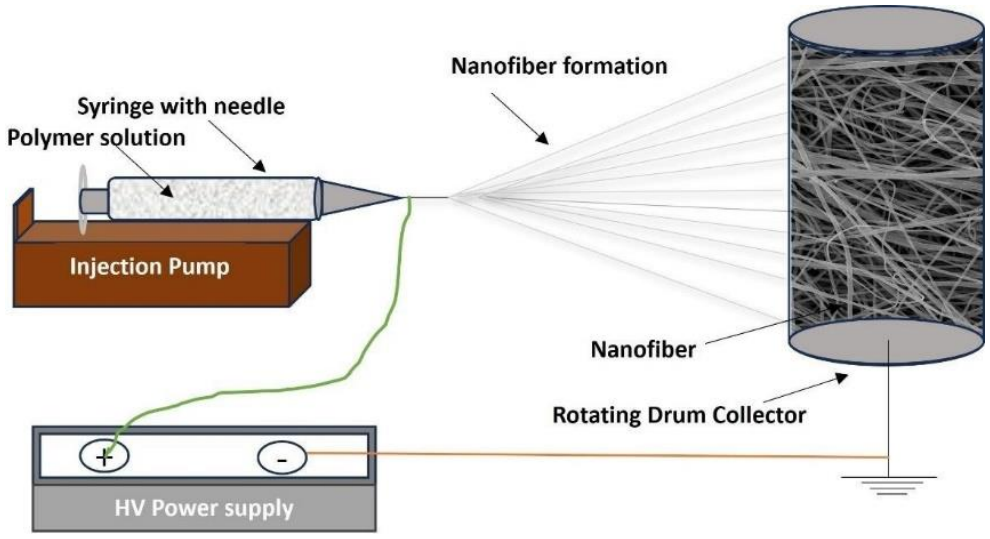


**Figure 1.** Schematic representation of the traditional electrospinning setup used for the fabrication of nanofibers.

Integrated Nano, 2024, Vol. X, Iss. X, 27-40
DOI: 10.62184/in.jin0101202422

Research Article

## 3. Characterization

Using a scanning electron microscope (SEM) (JEOL JSM-6010LV-SEM, Tokyo, Japan) with a 20 kV accelerating voltage, the surface morphology of the optimum PVDF-TPU nanofibrous membranes was investigated. After being deposited on carbon tape that was adhered to aluminium stubs, the electrospun nanofiber samples were platinum sputter coated. Using Image-J software (Madison, WI, USA), the mean diameter size of the nanofibers was determined. The response of these nanofibers to piezoelectric activity was examined using Fourier Transform Infrared (FTIR) spectroscopy, taking into consideration the beta sheet composition of the nanofibers. A FTIR spectrometer can be used to easily assess the sample's molecular fingerprint based on the functional groups that are present and how they interact. The transmittance spectra of PVDF nanofibers were generated using a Perkin Elmer FTIR spectrometer that has a scanning resolution of 5 $cm^{-1}$ over a range of 4100–400 $cm^{-1}$.

A piece of the same nanofiber mat sheet was tested for piezoelectric performance through the application of mechanical perturbation in the form of uniform airflow. The effect of airflow sensing and harvesting on the prototypes is tested by varying the velocity of airflow. The fabricated nanofiber membranes were sliced to the proper size of 2.5 x 2.5 cm. Then, they were placed between two sheets of aluminium foil that had insulated stainless steel wires attached to them. Using paper tape, the membrane comprised of aluminium foil sheets was assembled into a single unit, or nanofiber patch, as shown in Figure 2.

A piece of PVDF-TPU-based nanofiber membrane is also clearly shown in Figure 2, along with the nanofiber patch. The apparatus utilized to generate the wind flow consists of an electric air duster attached to a nozzle of radius 1 cm aimed towards the center of the PVDF or PVDF-TPU based sandwiched unit, as depicted in Figure 2.

Here, the airflow-based perturbation is applied to the sample vertically. The velocity of the airflow can be altered by adjusting the distance between the nozzle tip and the sample prototype. The velocity of airflow falling on the sample patch was measured using a velocity meter or anemometer included in the setup. The distance between the fan blade of the velocity meter and the tip of the air duster was measured with a ruler. Thus, the vertical distance between the fan blade and the tip of the air duster is fixed for each required velocity. The air duster was positioned at the appropriate height and directed towards the center of the sample for every airflow speed value. After exposing the sample to airflow for one second, the oscilloscope was used to measure the average of six separate peak-to-peak voltage measurements from the provided signal. A total of seven different speeds of airflow are reported, and the corresponding piezoelectric output voltage is measured for all four compositions, including pure PVDF and PVDF-TPU-based nanomembranes.

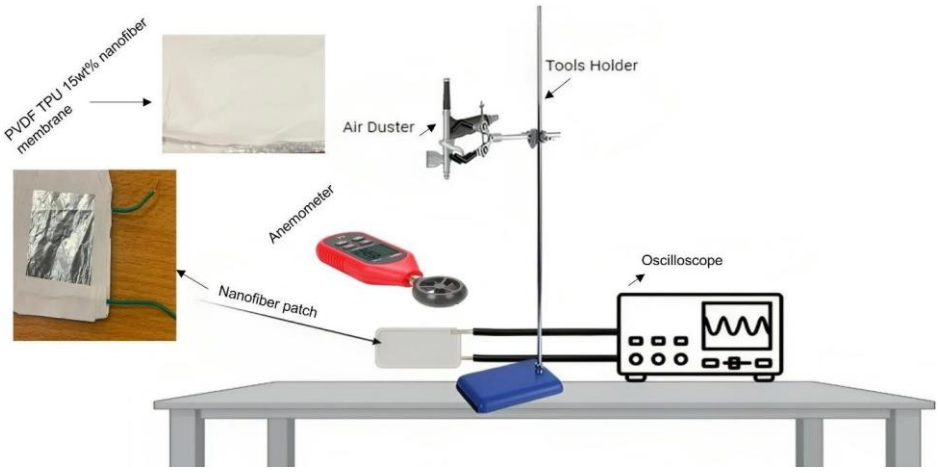


**Figure 2.** Experimental setup showing the airflow sensing-based analysis of PVDF-based nanofiber mat.

Integrated Nano, 2024, Vol. X, Iss. X, 27-40
DOI: 10.62184/in.jin0101202422

Research Article

## 4. Results and Discussion

The surface morphology of the generated electrospun nanofiber mat was studied using SEM. The corresponding image of the optimum composition of PVDF with 15 wt.% TPU is shown in Figure (3a). The matching fiber diameter distribution is displayed in Figure (3b), where the average diameter of the randomly distributed nanofibers is found to be around 370.23 nm.

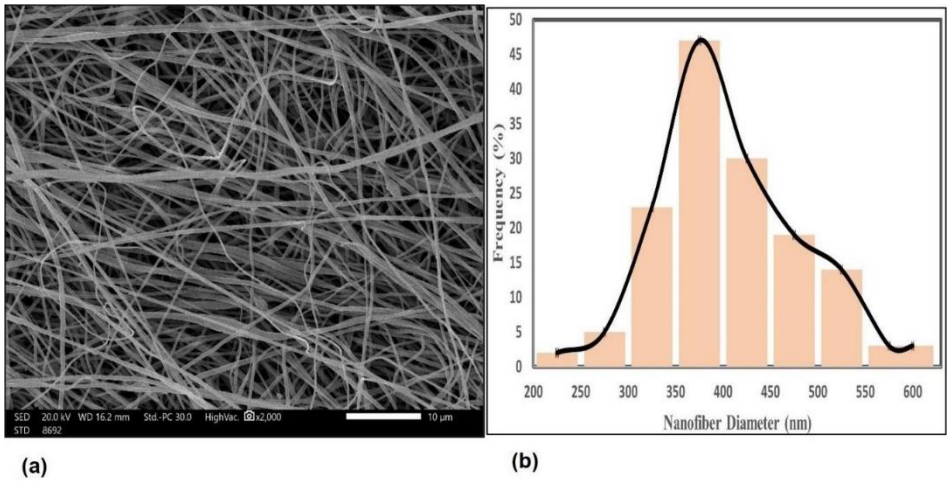


**Figure 3.** (a) SEM image of the fabricated PVDF-TPU 15 wt.% nanofiber mat at a scale bar of 10 µm and (b) histogram representing the corresponding fiber diameter distribution curve.

The β-sheet content associated with each composition can be calculated directly from the FTIR spectra shown in Figure 4. The FTIR spectra of PVDF make its crystalline phases quite evident. The primary electroactive polar phase of PVDF, which is responsible for its piezoelectric capabilities, is the β-phase, while the α-phase is the stable non-polar phase. Because of the alignment of induced dipoles under the influence of an electric field, the electrospinning process significantly increased the inherent β-phase. In relation to the crystal phase, the most prominent bands of PVDF are observed in the wavenumber range of 700 $cm^{-1}$ to 1500 $cm^{-1}$. Of these, the β-phase is clearly associated to the transmittance peaks at 840, 880, 1175, and 1275 $cm^{-1}$, and the α-phase is related to the peaks at 410, 489, 532, 614, 762, 796, 875, 976, 1210, and 1383 $cm^{-1}$. Several peaks linked to the "γ" phase may be found at 431, 482, 811, and 1234 $cm^{-1}$ [47]. The electroactive β-phase content for each composition can be calculated using Beer Lambert's law by measuring the intensity of absorbance bands at 760 $cm^{-1}$ and 840 $cm^{-1}$ and is given by:

$$\mathbf{f(\beta) = \frac{A_\beta}{1.26\,A_\alpha + A_\beta}} \qquad (2)$$

where $A_\beta$ and $A_\alpha$ represent the absorbance values at 840 $cm^{-1}$ and 760 $cm^{-1}$[44, 45].

The absorbance peak at 760 $cm^{-1}$, which corresponds to the crystalline α-phase, is caused by the $CF_2$ bending mode and the skeleton bending vibration mode of C(H)-C(F)-C(H). Similarly, the absorbance peak at 840 $cm^{-1}$ of the polar β-phase, owing to $CH_2$, shows a rocking vibrational band as well as C-C and $CF_2$ stretching. Two other peaks are recorded at 1175 $cm^{-1}$ and 1400 $cm^{-1}$, respectively, which correspond to the C-H and C-F vibrations [48–51]. The primary characteristic bands linked to TPU are located at 1533, 1735, 2971, and 3365 $cm^{-1}$. These peaks primarily correlate with the asymmetric bonds -CONH-, C=O, C-H, and N-H stretching, respectively [52, 53]. Certain nonpolar α-phase peaks, like 489, 614, 760, and 796 $cm^{-1}$ have diminished as a result of the TPU polymer's integration with

Integrated Nano, 2024, Vol. X, Iss. X, 27-40

DOI: 10.62184/in.jin0101202422

Research Article

PVDF; this is evident in the spectra. The transmittance peaks at 760 $cm^{-1}$ and 840 $cm^{-1}$ are marked in Figure 6. The decrease in the transmittance peak corresponding to 760 $cm^{-1}$ by the addition of TPU is visualized in Figure 4. Thus, by checking the absorbance values corresponding to 760 $cm^{-1}$ and 840 $cm^{-1}$ and applying in Beer Lambert's law gave us an idea about β-sheet content and crystallinity for each composition. The β-phase content percentages for pure PVDF, PVDF-TPU with 10 and 15 wt.% nanomat are roughly calculated to be 70.3%, 73.9%, and 80.4%, respectively, indicating the potential of PVDF-TPU-based nanomats for energy harvesting and sensing applications as depicted in Table 1. The mechanical flexibility of TPU, which helps to reposition electric dipoles inside the composite nanofiber when mechanical excitation is applied, accounts for 15 wt.% of TPU's high β-phase concentration [54].

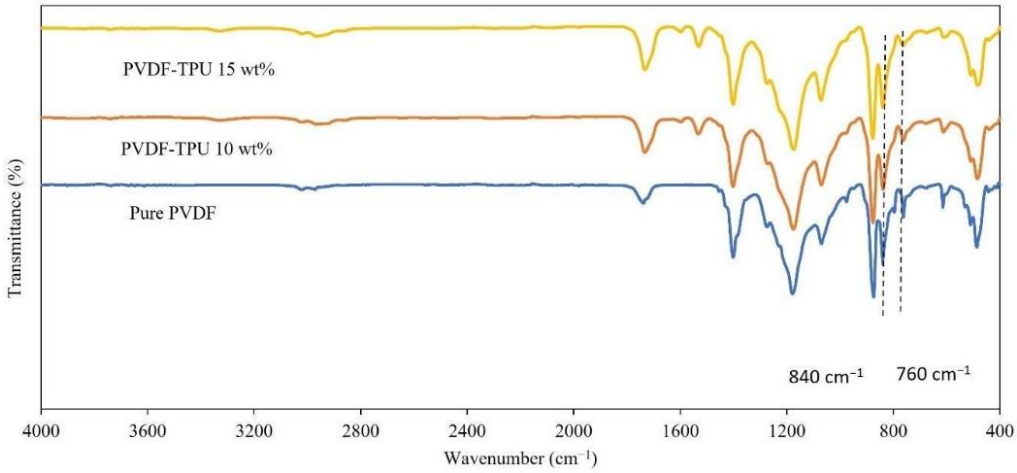


**Figure 4.** FTIR spectra of the electrospun piezo-active PVDF and PVDF-TPU-based nanomats.

**Table 1. The calculated β-phase content percentage of PVDF/TPU nanocomposite nanofibers.**

| Nanofiber Composition | β-Phase Content (%) |
|---|---|
| Pure PVDF | 70.3 |
| PVDF-TPU 10 wt % | 73.9 |
| PVDF-TPU 15 wt % | 80.4 |

The piezoelectric response enhancement of PVDF-based nanomats by the addition of TPU is confirmed by our previously published work [38, 43]. The additive TPU, which has higher mechanical elasticity than PVDF, greatly supports for the enhancement of piezoelectric activity. Thus, a piezoelastic membrane is constructed, and the mechanical elasticity of TPU provides an increase in flexibility for dipole excitations inside PVDF. Our earlier research, which focused on various PVDF-TPU blends, unequivocally demonstrated that the addition of TPU above specific threshold concentrations, such as 17.5%, reduced the composition's piezo-responsiveness. A detailed investigation of these compositions showed that the most effective piezoelectric membrane was obtained for concentrations of 15 wt.% and 17.5 wt.% of TPU with PVDF. As a result, the current study is restricted to PVDF with a TPU of 15 wt.% and doesn't test for a TPU at 20 wt.%, which will be weak according to our earlier findings [43]. However, the behaviour of PVDF-TPU-based nanomats towards perturbations associated with airflow is not yet reported. Present studies based on PVDF-TPU-based nanomats revealed a positive response towards airflow sensing and energy harvesting utilizing airflow. Among the four compositions, including pure PVDF and PVDF-TPU with 5, 10, and 15 wt.%, PVDF-TPU with 5 wt.% doesn't respond well to airflow-based perturbation. This clearly shows the inhibition of the piezoelectric activity of PVDF caused by the addition of TPU, and this matches our previously published piezo-characterization results. The PVDF-TPU with 5 wt.%

Integrated Nano, 2024, Vol. X, Iss. X, 27-40

DOI: 10.62184/in.jin0101202422

Research Article

didn't exhibit any piezoelectric response, showing the baseline only in the oscilloscope, and no enhancement from the baseline was observed. All three other samples sensed the airflow and piezoelectric voltage being generated. PVDF-TPU of 10 and 15 wt.% generated more voltage than the pure PVDF, showing the piezoelectric response enhancement behaviour of the composition. The piezoelectric voltage developed across the electrospun nanofiber mat is tabulated in Table 2.

**Table 2. Piezoelectric voltage with sensitivity values for different air flow velocities.**

| AirflowVelocity (km/h) | Pure PVDF | | PVDF-TPU 10 wt% | | PVDF-TPU 15 wt% | |
|---|---|---|---|---|---|---|
| | OutputVoltage (mV) | Sensitivity mV/ kmh$^{-1}$ | OutputVoltage (mV) | Sensitivity mV/ kmh$^{-1}$ | OutputVoltage (mV) | Sensitivity mV/ kmh$^{-1}$ |
| 6 ±1.5 | 31.3±1 | 3.85 | 35±1.2 | 4.71 | 54±1.9 | 4.76 |
| 9 ±1.5 | 43.7±1 | | 51±1 | | 70±0.1 | |
| 12 ±1.5 | 56.3±1 | | 66±1 | | 87±1.2 | |
| 15 ±1.5 | 62±1.2 | | 82.5±1.2 | | 99±1 | |
| 18 ±1.5 | 73.7±1 | | 92.5±1.2 | | 114±1.9 | |
| 21 ±1.5 | 82.5±1.2 | | 105±1.6 | | 129±1.8 | |
| 24±1.5 | 107.5±2 | | 126.2±2 | | 139±1 | |

The piezoelectric potential formed across the nanomat in response to the typical excitation force associated with airflow applied vertically is known as the sensitivity parameter. It is a measurement that shows the sample's piezoelectric reaction to the airflow and can be calculated from the slope of the velocity of airflow-voltage graph [46]. The relationship between the generated voltage and velocity of the airflow for the three compositions are shown in Figure 5. The plot clearly represents the enhancement in generated voltage occurred by the addition of TPU with 10 and 15 wt.%. Here, an electric potential is developed when the wind force or airflow-based force creates a stress in the nano-membrane and this perturbation is expressed out in the form of an electric potential [55]. PVDF-based nanomatsexhibited a sensitivity of 3.85 mV/kmh$^{-1}$. Similarly, PVDF-TPU with 10 and 15 wt.% showed a sensitivity of 4.71 mV/kmh$^{-1}$ and 4.76 mV/kmh$^{-1}$, respectively. This scenario of wind energy mainly deals with the dynamic mechanical energy conversion to electric energy and can be considered as a part of vibrational energy harvesting [56].

The PVDF-TPU with 10 and 15 wt.% showed almost the same sensitivity. These types of dedicated electrospun nanomats experience a dense dipole moment due to the high surface-to-volume ratio of their fibrillar structure, that greatly promotes the piezoelectric activity and the prototype. This results in the generation of voltage from both the small piece of nanomat and the weak force associated with uniform airflow. Time-based waveforms produced in response to the wind force for each composition at a specific airflow velocity of 24 km/h are displayed in Figure 6. As shown in Figure 6, the visual representation of the obtained pulsed waveform voltage for each composition is derived from the airflow perturbations. Furthermore, the increase in piezo-responsiveness obtained for PVDF-TPU composites is associated with the flexibility of the dipole excitations. The advantage of elastomeric properties such as flexibility in TPU greatly influenced the dipole excitations positively occurring inside PVDF, increasing the piezoelectric activity. The increase in piezoelectric activity of the primary material is associated with the increase in polar crystalline β-phase content. First of all, the electrospinning method itself has the ability to generate fabricated nanomaterials with enhanced β-

Integrated Nano, 2024, Vol. X, Iss. X, 27-40

DOI: 10.62184/in.jin0101202422

Research Article

phase content due to the application of an electric field during the phenomenon. Hence, it can give the effect of electric poling. In addition, the blending of TPU with PVDF greatly improved the electroactive β-sheet contents, which was displayed in the form of improved piezo-responsiveness [57].

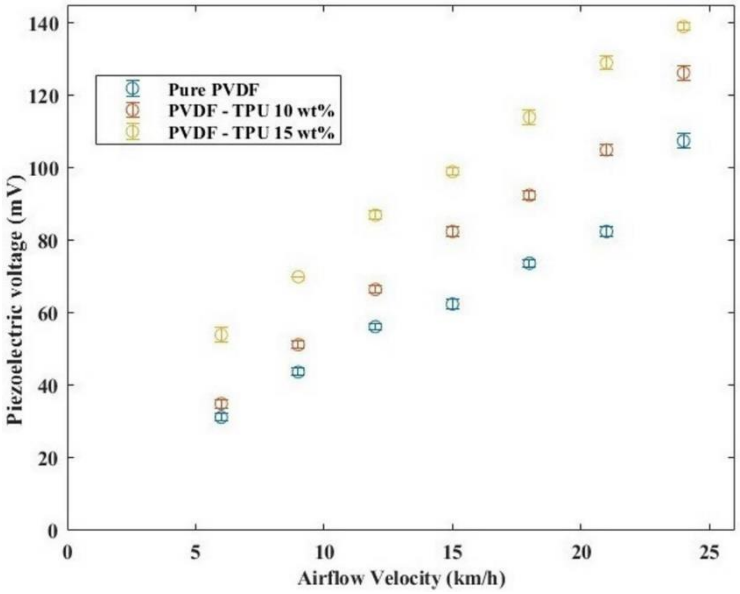


**Figure 5.** Relationship between peak-to-peak piezoelectric output voltage and airflow velocity.

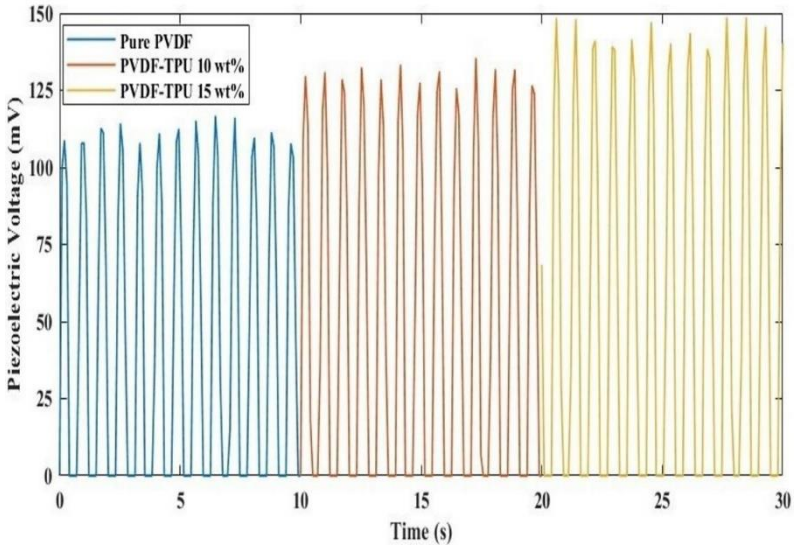


**Figure 6.** Airflow-based piezoelectric voltage waveform for pure PVDF and PVDF-TPU-based nanomats at 24 km/h airflow velocity.

## 5. Conclusion

Piezoelastic electrospun nanomats were fabricated to be applied in the fields of small-scale wind energy harvesting and airflow sensing. The focus was placed on examining how various airflow velocities affected the fabricated nanomats, where the sensitivity was examined. Piezoelectric voltage exhibits a positive linear trend as airflow velocities increases for three compositions of the tested samples. The incorporation of TPU to be blended in PVDF enhanced the sensing and energy harvesting performance towards environmental energy flow. An optimum

piezoelectric voltage of 139 ± 1 mV is developed across PVDF-TPU at 15 wt.% under the influence of an airflow velocity of 24 km/h. The β-sheet composition was found to be around 80% in the most successful prototype, which combined 15 wt.% of TPU and PVDF. The presented work effectively demonstrated piezoelectric energy harvester-based nanofibers that can sense and capture ambient airflow.

## Acknowledgement and Funding

The presented research work has been supported by Kuwait College of Science and Technology. The authors are grateful to Suresh Gyan Vihar University for providing us with the FTIR analysis.

## Conflicts of Interest

No potential conflicts of interest are reported by the authors.

## Author Information

**Corresponding Author:** Remya Nair*

**E-mail:** r.nair@kcst.edu.kw

## References

[1] Wei, Q., Xiong, F., Tan, S., Huang, L., Lan, E., Dunn, B., and Mai, L. (2017) Porous one-dimensional nanomaterials: design, fabrication and applications in electrochemical energy storage. Advanced Materials, 29, 1602300. https://doi.org/10.1002/adma.201602300.

[2] Zhang, T., Yang, T., Zhang, M., Bowen, C., and Yang, y. (2020). Review recent progress in hybridized nanogenerators for energy Scavenging. iScience, 23,101689. https://doi.org/10.1016/j.isci.2020.101689.

[3] Ellabban, O., Abu-Rub, H., and Blaabjerg, F. (2014). Renewable energy resources: current status, future prospects and their enabling technology. Renewable and Sustainable Energy Reviews, 39, 748. https://doi.org/10.1016/j.rser.2014.07.113.

[4] Selvan, K., and Ali, M. (2016). Micro-scale energy harvesting devices: review of methodological performances in the last decade. Renewable and Sustainable Energy Reviews, 54. https://doi.org/10.1016/j.rser.2015.10.046.

[5] Kiziroglou, M., and Yeatman, E. (2012) Materials and techniques for energy harvesting. Functional Materials for Sustainable Energy Applications, 541. https://doi.org/10.1533/9780857096371.4.539.

[6] Zhao, L.,and Yang, Y. (2017). Toward small-scale wind energy harvesting: design, enhancement, performance comparison, and applicability. Shock and Vibration, 2017, 1. https://doi.org/10.1155/2017/3585972.

[7] Zou, H., Cai, F., Zhang, J. ,and Chu, Z. (2022). Overview of environmental airflow energy harvesting technology based on piezoelectric effect. Journal of Vibroengineering, 24, 91. https://doi.org/10.21595/jve.2021.21979.

[8] Akin-Ponnle, A., and Carvalho, N (2021). Energy harvesting mechanisms in a smart city—a review. Smart Cities, 4, 476. https://doi.org/10.3390/smartcities4020025.

[9] Nie, G., Yao, Y., Duan, X., Xiao, L., and Wang, S. (2021). Advances of piezoelectric nanomaterials for applications in advanced oxidation technologies. Current Opinion in Chemical Engineering, 33, 100693. http://doi.org/10.1016/j.coche.2021.100693.

[10] Kapat, K., Shubhra, Q., Zhou, M., and Leeuwenburgh, S (2020). Piezoelectric nano-biomaterials for biomedicine and tissue regeneration. Advanced Functional Materials, 30, 1909045. https://doi.org/10.1002/adfm.201909045.

[11] Bairagi S., Islam S.-ul, Shahadat d M., Mulvihill D.M., and Ali W.,( 2023). Mechanical energy harvesting and self powered electronic applications of textile based piezoelectric nanogenerators: a systematic review. Nano energy, 111, 108414. https://doi.org/10.1016/j.nanoen.2023.108414.

[12] Zhang C., Fan W., Wang S., Wang Q., Zhang Y., and Dong K., (2021). Recent progress of wearable piezoelectric

nanogenerators. ACS Applied Electronic Materials, 3, 2449. https://doi.org/10.1021/acsaelm.1c00165.

[13] Li X., Sun M., Wei X., Shan C., and Chen Q. (2018). 1D piezoelectric material based nanogenerators: methods, materials and property optimization. Nanomaterials, 8, 188. https://doi.org/10.3390/nano8040188.

[14] Bonfim D. P. F., Cruz F. G. S., Guerra V. G., and Aguiar M. L. (2021). Development of filter media by electrospinning for air filtration of nanoparticles from pet bottles. Membranes, 11, 293. https://doi.org/10.3390/membranes11040293.

[15] Xue J., Wu T., Dai Y., and Xia Y., (2019). Electrospinning and electrospun nanofibers: Methods, materials, and applications. Chemical Reviews, 119, 5298. https://doi.org/10.1021%2Facs.chemrev.8b00593.

[16] Ruan L., Yao X., Chang Y., Zhou L., Qin G., and Zhang X. (2018). Properties and applications of the β phase poly(vinylidene fluoride). Polymers, 10, 228. https://doi.org/10.3390/polym10030228.

[17] Ebnesajjad S., (2011). Introduction to fluoropolymers, in Applied Plastics Engineering Handbook: Processing and materials. Elsevier, 49. https://doi.org/10.1016/B978-1-4377- 3514-7.10004-2.

[18] Alhasssan Z. A., Burezq Y. S., Nair R., and Shehata N., (2018). Polyvinylidene difluoride piezoelectric electrospun nanofibers: Review in synthesis, fabrication, characterizations, and applications. Journal of Nanomaterials, 8164185. https://doi.org/10.1155/2018/8164185.

[19] Mishra S., Unnikrishnan L., Nayak S. K., and Mohanty S., (2019). Advances in piezoelectric polymer composites for energy harvesting applications: a systematic review. Macromolecular Materials and Engineering, 304, 1800463. https://doi.org/10.1002/mame.201800463.

[20] Vijayakumar R. P., Khakhar D. V., and Misra A., (2010). Studies on α to β phase transformations in mechanically deformed PVDF films. J Applied Polymer Science, 117, 3491. https://doi.org/10.1002/app.32218.

[21] Sukumaran S., Chatbouri S., Rouxel D., Tisserand E., Thiebaud F., and Zineb T.Ben, . (2021). Recent advances in flexible PVDF based piezoelectric polymer devices for energy harvesting applications. J Intelligent Material Systems and Structures, 32, 746. https://doi.org/10.1177/1045389X20966058.

[22] Tanaka M., Tanaka Y., and Chonan S., (2008). Measurement and evaluation of tactile sensations using a PVDF sensor. J Intelligent Material Systems and Structures, 19, 35. https://doi.org/10.1177/1045389X06072802.

[23] Kalimuldina, G., Turdakyn N., Abay I., Medeubayev A. , Nurpeissova A., Nurpeissova A. , Adair D., and Bakenov Z., (2020). A review of piezoelectric pvdf film by electrospinning and its applications. Sensors, 20, 5214. https://doi.org/10.3390/s20185214.

[24] Luo H., and Hanagud S., (1999). Pvdf film sensor and its applications in damage detection. Journal of Aerospace Engineering, 12, 1. https://doi.org/10.1061/(ASCE)0893-1321(1999)12:1(23).

[25] Gu H., Zhao Y., and Wang M. L., (2005). A wireless smart PVDF sensor for structural health monitoring. Structural Control and Health Monitoring, 12, 329. https://doi.org/10.1002/stc.61.

[26] Shikida M., Shimizu T., Sato K., and Itoigawa K., (2003). Active tactile sensor for detecting contact force and hardness of an object. Sensors and Actuators A: Physical, 103, 213. http://doi.org/10.1016/S0924-4247(02)00336-9.

[27] Bian Y., Liu R., and Hui S., (2016). Fabrication of a polyvinylidene difluoride fiber with a metal core and its application as directional air flow sensor.

Functional Materials Letters, 9, 1. https://doi.org/10.1142/S1793604716500016.

[28] Bian Y., Liu R., Huang X., Hong J., Huang H., and Hui S., (2015). Design and fabrication of a metal core PVDF fiber for an air flow sensor. Smart Materials Structures, 24, 105001. http://doi.org/10.1088/0964-1726/24/10/105001.

[29] Hu J., Peng H., Mao T., Liu T., Guo M., Lu P., Bai Y., Zhao C., (2019). An airflow sensor array based on polyvinylidene fluoride cantilevers for synchronously measuring airflow direction and velocity. Flow Measurement and Instrumentation, 67, 166. http://doi.org/10.1016/j.flowmeasinst.2019.04.010.

[30] Berry R. B., Koch G. L., Trautz S., and Wagner M. H., (2005). Comparison of respiratory event detection by a polyvinylidene fluoride film airflow sensor and a pneumotachograph in sleep apnea patients. Chest, 128, 1331. https://doi.org/10.1378/chest.128.3.1331.

[31] Li Q., Xing J., Shang D., and Wang Y., (2019). A flow velocity measurement method based on a PVDF piezoelectric sensor. Sensors, 19, 1657. https://doi.org/10.3390/s19071657.

[32] Mhetre M. R., and Abhyankar H. K., (2017). Human exhaled air energy harvesting with specific reference to PVDF film. Engineering Science and Technology, an International Journal, 20, 332. https://doi.org/10.1016/j.jestch.2016.06.012 .

[33] Choi S.and Jiang Z., (2006). A novel wearable sensor device with conductive fabric and PVDF film for monitoring cardiorespiratory signals. Sensors and Actuators, A: Physical, 128, 317. https://doi.org/10.1016/j.sna.2006.02.012.

[34] Kryger M., Eiken T., and Qin L., (2013). The use of combined thermal/pressure polyvinylidene fluoride film airflow sensor in polysomnography. Sleep and Breathing, 17, 1267. https://doi.org/10.1007/s11325-013-0832-5.

[35] Zhang Y. Q. and Peng H. M., (2021). PVDF airflow sensor array based on the whistle cavity structure," in Proceedings of the 2020 15th Symposium on Piezoelectricity, Acoustic Waves and Device Applications, SPAWDA 2020, Institute of Electrical and Electronics Engineers Inc., 160. https://doi.org/10.1109/SPAWDA51471.2021.9445481.

[36] Akkaya Oy S., (2020). A piezoelectric energy harvesting from the vibration of the airflow around a moving vehicle. International Transactions on Electrical Energy Systems, 30, 12655. https://doi.org/10.1002/2050-7038.12655.

[37] Gee S., Johnson B., and Smith A. L., (2018). Optimizing electrospinning parameters for piezoelectric PVDF nanofiber membranes. Journal of Membrane Science, 563, 804. https://doi.org/10.1016/j.memsci.2018.06.050.

[38] Shehata N., Elnabawy E., Abdelkader M., Hassanin A. H., Salah M., Nair R., and Bhat S. A., (2018). Static-aligned Piezoelectric poly (vinylidene fluoride) electrospun nanofibers/ MWCNT composite membrane: facile method. Polymers, 10, 965. https://doi.org/10.3390/polym10090965.

[39] Choi, M., Murillo, G., Hwang, S., Kim, J., Jung, j., Chen, C., Lee, M. (2017). Mechanical and electrical characterization of PVDF-ZnO hybrid structure for application to nanogenerator. Nano Energy, 33, 462.https://doi.org/10.1016/j.nanoen.2017.01.062.

[40] Parangusan, H., Ponnamma, D., and Al-Maadeed, M. (2018). Stretchable electrospun PVDF- HFP/Co-ZnO nanofibers as piezoelectric nanogenerators. Scientific Reports, 8, 754. https://doi.org/10.1038/s41598-017-19082-3.

[41] Chamankar, N., Khajavi, R., Yousefi, A., Rashidi, A., and Golestanifard, F. (2020). A flexible piezoelectric pressure

sensor based on PVDF nanocomposite fibers doped with PZT particles for energy harvesting applications. Ceramics International, 46, 19669. https://doi.org/10.1016/j.ceramint.2020.03.210.

[42] Du, X., Zhou, Z., Zhang, Z, Yao, L., Zhang, Q., and Yang, H. (2022). Porous, multi-layered piezoelectric composites based on highly oriented PZT/PVDF electrospinning fibers for high-performance piezoelectric nanogenerators. Journal of Advanced Ceramics, 11, 331. https://doi.org/10.1007/s40145-021-0537-3.

[43] Elnabawy, E. Hassanain, A., Shehata, N., Popelka, A., Nair, R., Yousef, S., and Kandas, I. (2019). Piezoelastic PVDF/TPU nanofibrous composite membrane: Fabrication and characterization. Polymers, 11, 1634.https://doi.org/10.3390/polym11101634.

[44] Lin, T., Lou, C., and Lin, J. (2017). The effects of thermoplastic polyurethane on the structure and mechanical properties of modified polypropylene blends. Applied Sciences, 7, 1254. https://doi.org/10.3390/app7121254.

[45] Aurilia, M., Piscitelli, F., Sorrentino, L., Lavorgna, M., and Iannace, S. (2011) . Detailed analysis of dynamic mechanical properties of TPU nanocomposite: The role of the interfaces. European Polymer Journal, 47,925. https://doi.org/10.1016/j.eurpolymj.2011.01.005.

[46] Shehata, N., Nair, R., Boualayan, R, Kandas, I., Masrani, A., Elnabawy, E., Omran, N., Gamal, M., and Hassanin, A. (2022). Stretchable nanofibers of polyvinylidenefluoride (PVDF)/thermoplastic polyurethane (TPU) nanocomposite to support piezoelectric response via mechanical elasticity. Scientific Reports, 12, 8335. https://doi.org/10.1038/s41598-022-11465-5.

[47] Cai, X., Lei, T., Sun, D., and Lin, L. (2017). A critical analysis of the α, β and γ phases in poly(vinylidene fluoride) using FTIR. Royal Society of Chemistry Advances, 7, 15382, https://doi.org/10.1039/C7RA01267E.

[48] Sengupta, D., Kottapalli, A.,3, Chen, S., Miao, J., Kwok, C., Triantafyllou, M., Warkiani, M., and Asadnia, M. (2017). Characterization of single polyvinylidene fluoride (PVDF) nanofiber for flow sensing applications. AIP Advances, 7, 105205. https://doi.org/10.1063/1.4994968.

[49] Jana, S., Garain, S., Sen, S., and Mandal, D. (2015). The influence of hydrogen bonding on the dielectric constant and the piezoelectric energy harvesting performance of hydrated metal salt mediated PVDF films. Physical Chemistry Chemical Physics, 17, 17429. https://doi.org/10.1039/C5CP01820J.

[50] Kaspar P., Sobola, D., Částková, K., Knápek, A., Burda, D., Orudzhev, F., Dallaev, R., Tofel, P., Trcka, T., Grmela, L., and Hadaš, Z., (2020). Characterization of polyvinylidene fluoride (Pvdf) electrospun fibers doped by carbon flakes. Polymers, 12, 1. https://doi.org/10.3390/polym12122766.

[51] Mahato, P., Seal, A., Garain, S., and Sen, S. (2015). Effect of fabrication technique on the crystalline phase and electrical properties of PVDF films. Materials Science-Poland, 33, 157. https://doi.org/10.1515/msp-2015-0020.

[52] Gergeroglu, H., and Avcı, H. (2017). Functional composite nanofibers derived from natural extract of Satureja hortensis. Anadolu University Journal of Science and Technology-A Applied Sciences and Engineering, 18, 908. https://doi.org/10.18038/aubtda.339963

[53] Shaker, A., Hassanin, A., Shaalan, N., Hassan, M., and El-Moneim, A. (2019). Micropatterned flexible strain gauge sensor based on wet electrospun polyurethane/PEDOT: PSS nanofibers. Smart Materials and Structures, 28, 075029. https://doi.org/10.1088/1361-665X/ab20a2.

[54] Dai, Z., Feng, Z., Feng, C., Meng, L., Li, C., Wang, C., Han, L., Bai, Y. (2021). Thermoplastic polyurethane elastomer induced shear piezoelectric coefficient enhancement in

DOI: 10.62184/in.jin0101202422



bismuth sodium titanate – PVDF composite films. Journal of Applied Polymer Science, 138, e49818. https://doi.org/10.1002/app.49818.

[55] Naqvi, A., Ali, A., Altabey, W., and Kouritem, S. (2022). Energy harvesting from fluid flow using piezoelectric materials: A review. energies, 15, 7424. https://doi.org/10.3390/en15197424.

[56] Safaei, M., Sodano, H., and Anton, S. (2019). A review of energy harvesting using piezoelectric materials: State-of-the-art a decade later (2008-2018). Smart materials and structures, 28, 113001. https://doi.org/10.1088/1361-665X/ab36e4.

[57] Bertolini, M., Zamperlin, N., Barra, G., and Pegoretti, A. (2023). Development of poly(vinylidene fluoride)/thermoplastic polyurethane/carbon black-polypyrrole composites with enhanced piezoelectric properties. SPE Polymers, 4, 143. https://doi.org/10.1002/pls2.10097.